PCCP

PAPER

Cite this: *Phys. Chem. Chem. Phys.*, 2015, **17**, 29935

pH-responsive ion transport in polyelectrolyte multilayers of poly(diallyldimethylammonium chloride) (PDADMAC) and poly(4-styrenesulfonic acid-*co*-maleic acid) (PSS-MA) bearing strong- and weak anionic groups†

Eliana Maza,[a] Jimena S. Tuninetti,[a] Nikolaos Politakos,[b] Wolfgang Knoll,[c] Sergio Moya[b] and Omar Azzaroni*[a]

Received 8th July 2015,
Accepted 4th October 2015

DOI: 10.1039/c5cp03965g

www.rsc.org/pccp

The layer-by-layer construction of interfacial architectures displaying stimuli-responsive control of mass transport is attracting increasing interest in materials science. In this work, we describe the creation of interfacial architectures displaying pH-dependent ionic transport properties which until now have not been observed in polyelectrolyte multilayers. We describe a novel approach to create pH-controlled ion-rectifying systems employing polyelectrolyte multilayers assembled from a copolymer containing both weakly and strongly charged pendant groups, poly(4-styrenesulfonic acid-*co*-maleic acid) (PSS-MA), alternately deposited with poly(diallyldimethylammonium chloride) (PDADMAC). The conceptual framework is based on the very contrasting and differential interactions of PSS and MA units with PDADMAC. In our setting, sulfonate groups play a structural role by conferring stability to the multilayer due to the strong electrostatic interactions with the polycations, while the weakly interacting MA groups remain ''silent'' within the film and then act as on-demand pH-responsive units. When these multilayers are combined with a strong cationic capping layer that repels the passage of cationic probes, a pH-gateable rectified transport of anions is observed. Concomitantly, we also observed that these functional properties are significantly affected when multilayers are subjected to extensive pH cycling as a consequence of irreversible morphological changes taking place in the film. We envision that the synergy derived from combining weak and strong interactions within the same multilayer will play a key role in the construction of new interfacial architectures displaying tailorable ion transport properties.

Introduction

The fabrication of polymer thin films with precisely defined and tunable functions incorporated into their physical domains has been the subject of intensive research during the last decade. Within this context, the layer-by-layer (LbL) adsorption technique emerged as an alternative ''bottom-up'' approach exploiting the self-assembly of diverse building blocks by noncovalent interactions, thus providing a low cost and facile way to create sophisticated multilayered interfacial architectures with the potential of integrating a broad variety of functional units into the film. This technique was first proposed by Iler in 1966,[1] and then rediscovered by Decher and Hong in 1991,[2] and is based on the alternate deposition of polyanions and polycations on a charged surface in order to form polyelectrolyte multilayers with nanometer-level control over the structure, composition, and properties.[3] Today this technique has taken on a new dimension,[4,5] as can be seen by the increasing number of applications of LbL assemblies in, namely photodiodes,[6] optical devices,[7] filtration membranes,[8] self-supported membranes with highly enhanced Young's moduli,[9] fuel cell membranes,[10] drug[11] and biomaterial[12] release systems, or biologically active coatings.[13]

Intensive research by different groups demonstrated that the properties of these assemblies depend on several conditions including polymer type and concentration,[14–16] molecular weight,[17–20] salt type and concentration,[21–26] and pH (when weak polyelectrolytes are involved).[27–31] In addition, it has been shown that the properties of the films depend on the nature of the outermost assembled layer.[29] Shiratori and Rubner[28]

[a] *Instituto de Investigaciones Fisicoquímicas Teóricas y Aplicadas (INIFTA), Universidad Nacional de La Plata (UNLP), CONICET, (1900) La Plata, Argentina. E-mail: azzaroni@inifta.unlp.edu.ar; Web: http://softmatter.quimica.unlp.edu.ar*
[b] *Biosurfaces Unit, CIC biomaGUNE, Paseo Miramón 182, 20009 San Sebastian, Gipuzkoa, Spain*
[c] *Austrian Institute of Technology GmbH, Donau Strasse 1, Vienna, Austria*

† Electronic supplementary information (ESI) available. See DOI: 10.1039/c5cp03965g

This journal is © the Owner Societies 2015

described how the thickness of polyacrylic acid/poly(allylamine hydrochloride) (PAA/PAH) films depends on the charge density of both polymers in solution, observing that thicker films are observed when both polymers are charged. In the case of weak polyelectrolytes it is possible to control the film properties by changing the pH of the polymer solution. Fujii *et al.*[32] described the dependence of the film thickness and roughness on the assembly pH. It has been reported that charge densities of the polymers changed when they are assembled in response to the immediate environment.[19] Even the degree of coiled or extended conformations of the polymers in solution changes during the deposition steps due to interaction with the polyelectrolytes assembled previously. In general, the degree of ionization of weak polyacids in films is higher than that in solution[20,33] due to ionization produced by the positively charged polyelectrolyte. The proportion in which the degree of ionization increases relative to the value in solution depends on the other polyelectrolyte in the assembly. Nevertheless, the pH and ionic strength conditions of the starting solutions are essential to obtain films with different characteristics. Caruso's group gave an interesting twist to this framework through the multilayer assembly of an anionic copolymer, poly(4-styrenesulfonic acid-*co*-maleic acid) (PSS-MA), which consists of strongly charged styrene sulfonate (SS) groups and weakly charged maleic acid (MA) groups, together with PDADMAC, demonstrating that these multilayers are very stable over a wide range of pH.[20] On top of this, very recently, Moya and co-workers[34] reported interesting results indicating that interactions between carboxylate units and PDADMAC are anomalously weak and play no role in the electrostatic build-up of multilayers. This suggests that PSS-MA constitutes an anionic polyelectrolyte with very contrasting and differential interactions in the presence of PDADMAC as a counter-polyelectrolyte. Exciting opportunities to exploit synergies are revealed when we think in this manner. The presence of strong sulfonate groups can result in enhanced stability due to electrostatic interaction with quaternary amines of the polycations, while the weakly charged MA groups may potentially remain "silent" within the film and then act as pH-responsive units. In this sense, the involvement of "silent" charges in the modulation of film properties is still an unexplored scenario, which offers an interesting gamut of opportunities for creating interfacial assemblies displaying pH-switchable ion transport. In recent years there has been increasing interest in engineering the permeation properties of LbL assemblies with the aim of creating smart ion separation membranes.[35] These studies predominantly focused on the permeation properties of linearly growing films such as PSS/PAH[36] or PSS/PDADMAC.[37] As a general trend, the ion transport properties of compact multilayers, in which the internal structural equilibrium is governed by "intrinsic" charge compensation, are rather poor. In this regard, Farhat and Schlenoff demonstrated that permeability could be increased by assembling the polyelectrolytes from solutions of higher ionic strength.[38] However, the same authors also demonstrated that PSS/PDADMAC multilayers assembled under saline conditions lead to strongly impermeable films with potential applications as anticorrosive coatings.[39] In a similar vein, interesting studies on the use of polyelectrolyte multilayers whose permeation properties can be switched by environmental pH changes have also been reported.[40,41] However, these approaches demanded the additional use of covalent interactions to stabilize the film because the pH-induced alterations of electrostatic interactions compromised the structural integrity of the multilayer.[42] In comparison to the number of studies performed with linearly growing multilayers assembled under low ionic strength conditions, up to now only a limited number of reports focused on the manipulation of permeability properties in exponentially growing multilayers.[43]

To date, despite the promising functional features of weak–strong copolymer polyelectrolyte multilayers, only a few detailed scientific studies on the matter have been carried out.[20,44,45] Even more important, the application of their appealing pH-switchable properties combining weak and strong moieties to control ion transport processes through "silent" charges remains fully unexplored. Taking into account these insights from previous studies and being aware of the potential impact of PSS-MA multilayers on the molecular design of responsive polymer films, we decided to explore this new conceptual paradigm based on the use of "silent" charges that do not participate in the electrostatic assembly to control the permeation of charged species. In the present work, we report the effectiveness of this all-supramolecular strategy to create pH-switchable, ion-rectifying interfaces operating under different pH and saline conditions without requiring further covalent chemistries to consolidate and stabilize the film.

Results and discussion

The deposition process of PSS-MA and PDADMAC was monitored *in situ* by surface plasmon resonance spectroscopy (SPR) in order to estimate surface coverage and thickness of the polyelectrolyte multilayer. Fig. 1 shows the dependence of the PSS-MA/PDADMAC multilayer growth on pH and ionic strength. The growth exhibited a marked supralinear, exponential-like behaviour in all cases except for assembly solutions in the absence of added salt. The exponential growth can be ascribed to the "in and out" diffusion of the assembled polyelectrolytes through the film, resulting in film rearrangement during the assembly process.[46–50] The linear or exponential growth mode depends on the strength of the intermolecular interactions of the polymers involved. These interactions are influenced or affected by the deposition conditions, such as salt concentration or solution pH.[51] In our case, the polyelectrolytes and the conditions employed for the assembly process favored the exponential growth of the films. The tendency of assembly growth at different pH values was strongly dependent on the presence of salt in the polyelectrolyte solutions. In the case of salt-free assembly solutions we observe that an increase in pH leads to thinner films. For example, the thickness of a PSS-MA/PDADMAC film containing 20 layers varies from 33 to 8 nm upon increasing the pH of the assembly solution from 3.5 to 9.5. This observation is in agreement with the previous results demonstrating that a decrease in film

 This journal is © the Owner Societies 2015

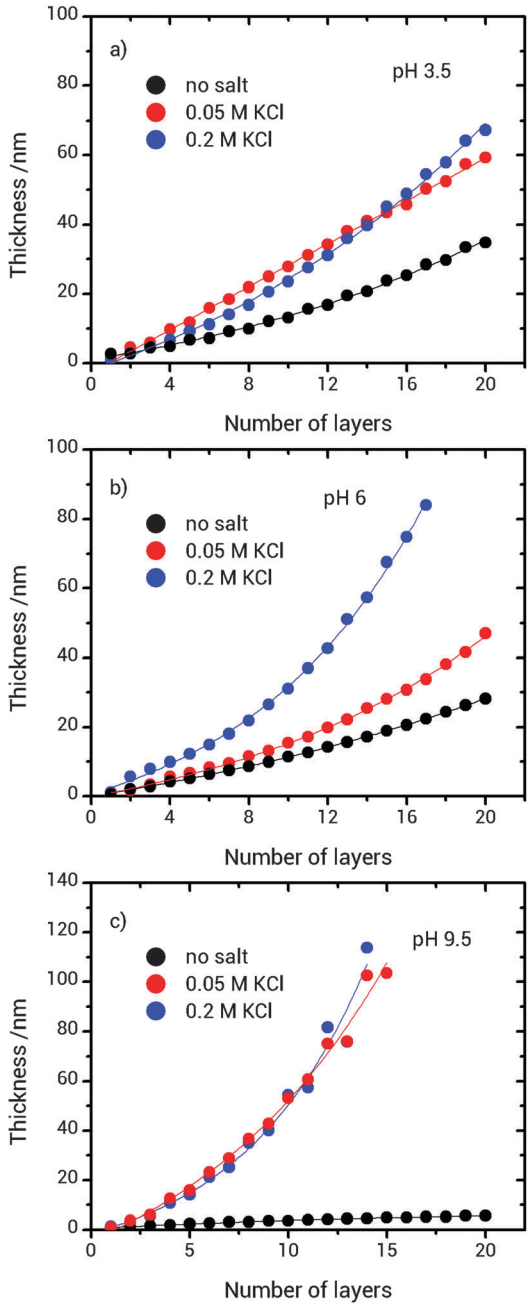

Fig. 1 Thickness evolution of (PSS-MA/PDADMAC)$_n$ films as a function of the number of deposited layers at pH (a) 3.5, (b) 6, (c) 9.5. Odd layers are from PSS-MA and even layers are from PDADMAC.

thickness is typically observed when the charge density of the polymer is increased.[27,28] However, this trend is fully reversed upon adding salt to the assembly solution. A dramatic increase in supralinear growth behavior, and consequently in thickness, is observed in the presence of 0.05 and 0.2 M KCl. Under each particular pH condition the film became thicker with the increase in KCl content. We should consider that the higher the KCl concentration, the higher the coverage of polyelectrolyte deposited, which is necessary to achieve the compensation of the surface charges due to the screening effect of the KCl ions on the polyelectrolyte charges.[52] The effect of pH on transition from linear to supralinear growth of polyelectrolyte multilayers has been studied in detail by several authors;[53] however, the influence of salt on this transition has been studied to a much lesser extent.[54]

For instance, a closer inspection of Fig. 1 indicates that at a particular ionic strength the assembly growth does not follow the same tendency with pH. Without the addition of salt the thickness decreased with the increase in pH; at 0.2 M KCl the behavior was quite the opposite, the thickness increased with the increase in pH, and at 0.05 M KCl there is no clear trend upon varying the pH, *i.e.* upon varying the pH from 3.5 to 5 little change in thickness was evidenced. Hence, for the sake of clarity, the behavior with pH at different ionic strengths was analyzed separately. For that purpose it was necessary to consider the change in the ionization degree of PSS-MA in regard to the pH of the solution while PDADMAC is always positively charged.

As mentioned before, without addition of salt the tendency of the assembly was similar to that found by other authors.[55] The charge density and the structural conformation of PDADMAC remain the same regardless of the pH. On the other hand, the higher the pH the more dissociated the carboxylic acid groups of PSS-MA and the higher the repulsive forces among the charges, causing a more extended conformation of the polymer chains. At lower pH there was less charge density and, as a consequence, the chains of PSS-MA adopted a more coiled conformation. As a result of the low charge density at low pH, more mass of PSS-MA was required to achieve surface charge compensation. In the same way, with the increase in pH the higher charge density was responsible for less quantities of polymer to achieve the charge compensation of the film already assembled.

At 0.2 M KCl the thickness increased upon increasing the pH conditions. This behavior agrees with the fact that at higher pH values PSS-MA is highly charged and, consequently, the electrostatic attraction between PSS-MA and PDADMAC is stronger. Considering this perspective, under low pH conditions the charge density of PSS-MA was low and then for the adsorption of the next layer PDADMAC was not necessary to be in great quantities for charge compensation. In contrast, when the pH was high the charge density of PSS-MA was higher and more quantities of PDADMAC were assembled. This would occur in the same manner throughout the entire assembly process. The mass of the material and, therefore, the thickness of a new layer deposited depend on the charge density of the film assembled previously. On the other hand, the presence of salt produced a screening effect on the polymer charges but this effect was more significant when there was greater charge density in both assembled polymers. The salt always affected in the same way as PDADMAC, regardless of the pH of the assembly solution. However, the influence on PSS-MA was higher as the pH increased due to the increase of the charge density of the polymer. Only the change in the ionic strength of the assembly solutions was important enough to reverse the tendency of the observed thicknesses of the films as the pH increased. In other words, the opposite trends of thicknesses observed in the absence and in the presence of salt upon changing the pH conditions

demonstrate the relevant role that the ionic strength plays in the growth behavior of the films.

The exponential growth of the multilayers in the presence of added salt at different pH values can be interpreted considering the delicate interplay between polymer interdiffusion and charge density of the polymer chains. It is well known that polyelectrolytes adsorbing on an oppositely charged surface experience both an electrostatic attraction to the surface (favoring adsorption) and an electrostatic repulsion within the layer (counteracting adsorption). For instance, when highly charged polyelectrolytes are adsorbed onto an oppositely charged surface, they are adsorbed rather flat and form thin layers due to strong repulsion between segments. If this repulsion is screened by adding salt, the adsorbed amount increases and the adsorbed layer becomes thicker.[56] However, this effect does not explain the supralinear growth observed in the presence of salt.

The so-called "exponential" or "supralinear" growth is typically observed when large interdiffusion takes place within the assembly and diffusion of polyelectrolyte chains within a swollen LbL film is coupled with reversible or irreversible exchange with chains that are already a part of the assembly. In our case, the addition of salt to the assembly solution facilitates polyelectrolyte interdiffusion within the multilayered films, as has been conclusively demonstrated by Jomaa and Schlenoff in a set of neutron reflectivity experiments, and concomitantly leads to the exponential growth of the multilayer.[57]

Then, in addition to ionic strength, PSS-MA ionization as a function of pH also plays a role in the exponential growth of the multilayers. In principle, at low pH values the lower degree of acid ionization in MA would be reflected by a lower number of ionic cross-links with PDADMAC, thus resulting in an LbL film with a looser network, thus making it easier for polymer chains to penetrate the film. The enhancement of polyelectrolyte chain mobility/interdiffusion within the multilayer by altering the fraction of charged groups in the film has been demonstrated by Hammond's group. These authors demonstrated that a number of weak polycations are capable of interdiffusion and exchange with other polycations when the degree of ionization is close to 70%, with interdiffusion significantly more favorable when the degrees of ionization are lower than this threshold value.[58]

It is interesting to note that, in our present system, we observe a rather linear growth of PSS-MA/PDADMAC multilayers at pH 3.5 even in the presence of salt, which is therefore opposite to the observations of Hammond and co-workers. This strongly suggests that other additional factors hinder the interdiffusion of polyelectrolytes within the film. To understand these intriguing results we need to consider recent findings reported by Moya and co-workers on the formation of polyacrylic acid (PAA) and PDADMAC multilayers under acidic conditions.[34] These authors showed that PAA/PDADMAC multilayers display a marked growth pattern at pH 3 whereas for pH values higher than 6, the multilayer formation is drastically inhibited. Their isothermal titration calorimetry experiments provided surprising results: at pH 3, under conditions where carboxylate groups are fully protonated, titration was exothermic as expected due to the formation of complexes from oppositely charged polyelectrolytes (molar heat $\sim$2.11 kJ mol^{-1}); in contrast, at pH 13 (fully ionized carboxylate groups) almost no observable heat of reaction was measured, $\sim$0.048 kJ mol^{-1}. The highly reduced complexation heat at pH 13 is indicative of polymers that are not interacting, although PAA is fully charged and the electrostatic interaction should be at maximum. Conversely, at pH 3 the mixture of both polyelectrolyte solutions resulted in the instantaneous formation of interpolymer PAA–PDADMAC complexes.[59,60] Referring back to our results, we hypothesize that the strong interaction between the protonated carboxylate units in PSS-MA and PDADMAC is responsible for inhibiting the interdiffusion between polymer layers with the concomitant effect on the multilayer growth mode, structure and solvent content. In this context, we should also consider that inter- and intra-polyelectrolyte hydrogen bonding in PSS-MA layers might also take place within the assembly with its concomitant influence on the film grown.

Solvent can be trapped in cavities within a polyelectrolyte multilayer, either between polyelectrolyte molecules forming a given layer or between subsequent layers during assembly.[61] Little is known about how the water content evolves during the sequential deposition of the polyelectrolyte layers. This is an important concern in LbL films provided that the water content of the multilayer controls the local molecular interactions and determines key properties like permeability.[62] Hence, to reach a more comprehensive and realistic view of the physicochemical characteristics of the system under study we investigated the influence of the assembly conditions on the water content of the polyelectrolyte multilayer.

In contrast to SPR that is sensitive to differences in the optical density between the adsorbate and the bulk solution, *i.e.* it essentially senses the adsorbate mass, the quartz crystal microbalance technique with dissipation (QCM-D) is based on an entirely different transducer principle, namely, on the variation in the electromechanical response of a shear-oscillating piezoelectric sensor caused by polyelectrolyte adsorption. The quartz crystal microbalance with dissipation monitoring (QCM-D) has proven to be a powerful technique to follow the growth of polyelectrolyte multilayers and to characterize the mechanism of their assembly.[63] Owing to its acousto-mechanical transducer principle, the QCM-D technique is sensitive not only to the adsorbed molecules but also to the solvent that is retained within or hydrodynamically coupled to the surface-bound film. As a consequence, the mass obtained by QCM-D measurements corresponds to the total mass coupled to the motion of the sensor crystal, including both the mass of the polyelectrolytes, measured by, for example, SPR and the water bound to or dynamically coupled to the film. Therefore, the difference between the mass obtained from QCM measurements, m_{QCM}, and the mass obtained *via* SPR measurements, m_{SPR}, when operated in aqueous solution, provides a good estimate of the water content of the polyelectrolyte multilayer (see the ESI,† for details).

We observed that hydration of the PSS-MA/PDADMAC multilayers is strongly affected by the salt content of the assembly solution. It is known that the ionic strength has a direct impact

 This journal is © the Owner Societies 2015

on the conformation of the assembled layers. In stark contrast to the behavior of PSS/PDADMAC multilayers that behave as swollen polymer matrices that lose water as the ionic strength increases we found that PSS-MA/PDADMAC assemblies behave quite the opposite. In addition, we also found that pH plays an important role in tailoring the water content of the multilayer (Fig. S4 in ESI†). At pH 3.5 the water content steadily decreases during the multilayer assembly regardless of the ionic strength of the assembly solution. The presence of salt results in more hydrated films with water contents close to 60% after assembling 20 layers (see Fig. S4 in ESI†). Indeed, the water in the multilayer is not only the water associated to the monomer units of the polyelectrolytes, but also water which is entrapped between the polymer chains. In the absence of salt the polyelectrolytes adsorb on the surface adopting very flat conformations, and consequently this results in more compact and less hydrated films. In the presence of salt the fraction of segments in loops and tails become larger, thus leading to an increase in entrapped water. The morphology of these films prepared in the presence and in the absence of salt was examined by using AFM considering PDADMAC or PSS-MA as capping layers (Fig. 2). The surface roughness is markedly lower for multilayers terminated in PDADMAC layers regardless of the salt content of the assembly solution. Both films were smooth and uniform, with a root-mean-square roughness of *ca.* 0.3–0.4 nm (see Table 1). In the case of PSS-MA-capped films AFM imaging revealed the presence of globules of diameters ~70 nm and ~300 nm for films prepared without and with added salt, respectively. It is evident that the presence of PSS-MA in the capping layer leads to morphological changes and influences the surface texture resulting in rougher films.

At pH 6 the incorporation of water in the film during the sequential adsorption of polyelectrolyte multilayers was strongly affected by the presence of salt in the assembly solution. During the first five layers no significant differences between systems assembled in the presence or in the absence of salt were observed (see Fig. S4 in ESI†). Though after assembling the fifth layer films constructed in the presence of salt showed an increase in water content that reached a plateau after incorporating the 15th layer whereas those assembled in pure water described an almost

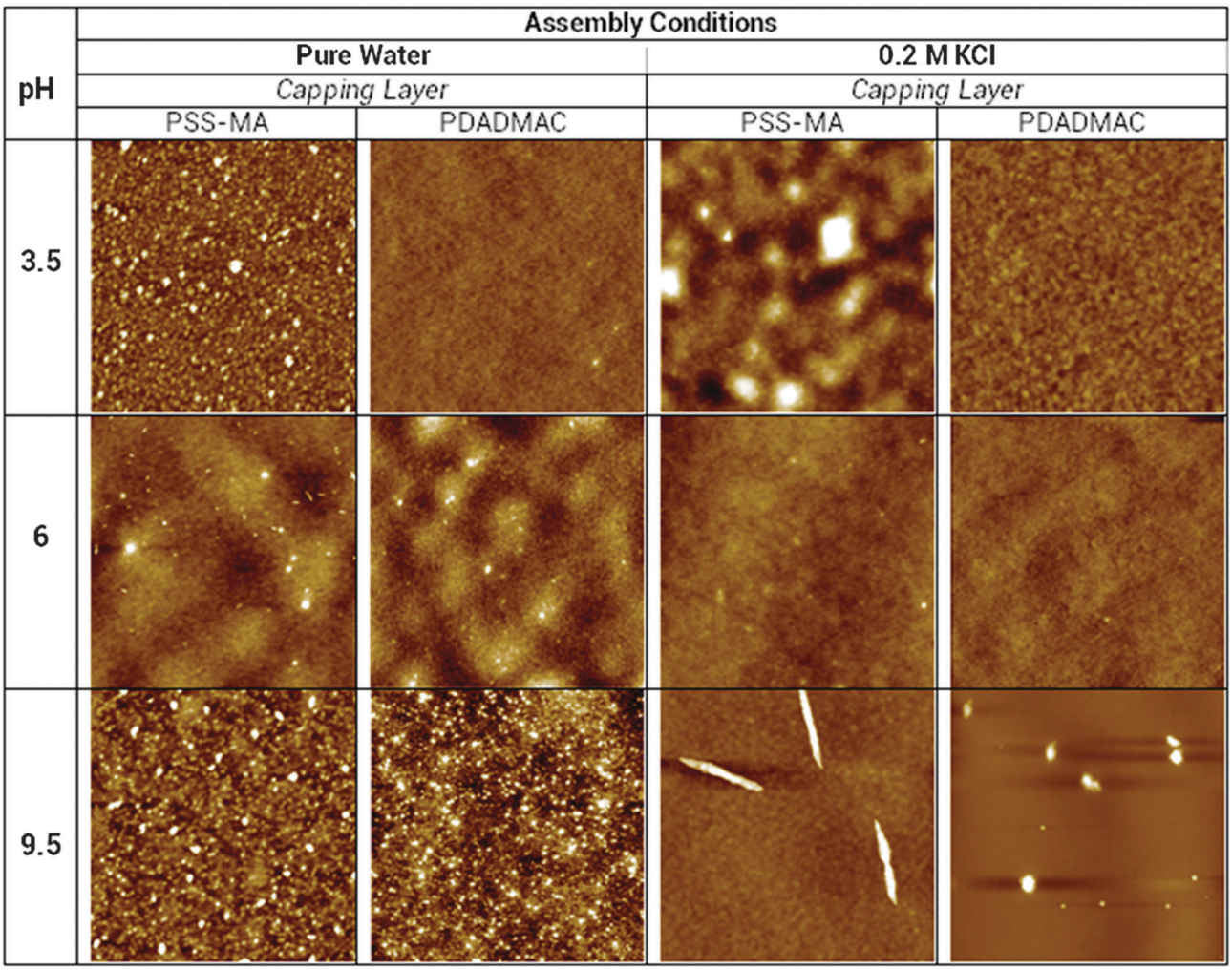

Fig. 2 Atomic force microscopy imaging (5 × 5 μm^2) of (PSS-MA/PDADMAC)$_9$PSS-MA ("PSS-MA capping layer") and (PSS-MA/PDADMAC)$_{10}$ ("PDADMAC capping layer") multilayers assembled in pure water and in the presence of 0.2 M KCl under different pH conditions.

Table 1 Root-mean-square (rms) surface roughness of (PSS-MA/PDADMAC)$_9$PSS-MA ("PSS-MA capping layer") and (PSS-MA/PDADMAC)$_{10}$ ("PDADMAC capping layer") multilayers assembled in pure water and in the presence of 0.2 M KCl under different pH conditions. Values are expressed in nanometers

	Assembly conditions			
	Pure water		0.2 M KCl	
	Capping layer		Capping layer	
pH	PSS-MA	PDADMAC	PSS-MA	PDADMAC
3.5	7.9	0.3	3.2	0.4
6	0.7	0.7	0.5	0.5
9.5	3.2	1.4	1.7	3.7

linear decrease in hydration until reaching a scenario close to dehydration. It is evident that the exponential behavior of the multilayer has an effect on the hydration properties provided that differences in water uptake come into light during the early stages of the supralinear growth, *i.e.* 5th–7th layer. At this pH the PSS-MA polyelectrolyte is not fully charged and the presence of salt may lead to the interpenetration of layers and the generation of amorphous polymeric domains, with this scenario being compatible with the formation of a hydrogel-like layer with considerable amounts of solvent. Interestingly, texture assessment by AFM revealed that, in contrast to observations at pH 3.5, the topographic characteristics of both type of films are independent of the nature of the capping layer and the multilayer assembly in the presence of 0.2 M KCl results in smoother films than in the absence of salt. Notably, the root-mean-square roughness of (PSS-MA/PDADMAC)$_{10}$ multilayers is below 0.5 nm, thus indicating the presence of an ultra-smooth film that is growing in a nonlinear fashion. This observation is not trivial provided that exponentially grown multilayers typically show the evolution of local inhomogeneities that ultimately leads to an increase in roughness (see Table 1).[64] In addition, these results suggest that for the PSS-MA/PDADMAC system the nonlinear growth cannot be due to an increase of the film roughness during buildup as suggested in the literature for other systems.[65]

The qualitative behavior of water uptake was fully reversed at pH 9.5 as much as the subsequent assembly after the seventh layer in the presence of 0.05 M KCl leads to films exhibiting lower water content as compared with those obtained in pure water, *i.e.* multilayer hydration without salt was higher than that under saline conditions. We inferred that this film was comparatively more compact than that assembled in pure water. This observation can be attributed to the fact that at pH 9.5 the PSS-MA is fully ionized and stronger electrostatic interactions can lead to better packing of the polyelectrolyte coils. It is worth mentioning that contraction of the coils may occur if the attractive intermolecular interactions become larger than the interaction with the solvent molecules. In extreme cases, the solvent is forced out of the polymer coil and the chain segments start to form compact aggregates.[66]

AFM imaging of these samples revealed significant differences between films prepared in pure water and salt-containing solutions (Fig. 3). (PSS-MA/PDADMAC)$_{10}$ multilayers prepared in pure water at pH 9.5 display a highly granular morphology that is hardly affected by the presence of PDADMAC or PSS-MA in the capping layer, even though PSS-MA-capped films display a slightly higher surface roughness.

In sharp contrast, (PSS-MA/PDADMAC)$_{10}$ multilayers assembled in 0.2 M KCl exhibit the presence of "wrinkles" or discrete "nanoaggregates" on top of considerably smooth surfaces depending on the presence of PSS-MA or PDADMAC, respectively, as the capping layer. The presence of wrinkles resembles those observed in PDADMAC/PSS multilayers grown under saline conditions resulting from the reorganization of the outer layers with the consequent increase in surface roughness (see Table 1). A similar morphological feature was also reported by Caruso *et al.*[67] in multilayers constituted of pH-sensitive copolymers comprising block domains of acrylic acid (AA) and styrene sulfonate (SS) groups (PAA$_x$-*b*-SS$_y$) and poly(allylamine hydrochloride) (PAH).

Referring back to hydration we need to note that after assembling the first layers hydration start to oscillate between about 30% and 70%, upon the assembly of PSS-MA and PDADMAC, respectively. The global structure of sufficiently thick polyelectrolyte multilayers has previously been conceptualized by a three-zone model: two interfacial zones, which are affected by the presence of the solid support and the bulk solution, respectively, and maintain a constant thickness; and an interior zone, placed between the two interfacial ones, which grows in thickness as additional layers are deposited. The change in the water content when passing from even to odd layers suggests that at least some of that water must be present in the interfacial zone adjacent to the bulk solution. Then, the differences in water content between multilayers with PDADMAC or PSS-MA as capping layers might be due to the particular hydration or reorganization of the outermost layers. Clearly, the presence of salt retains the polyelectrolytes in a strongly collapsed state inside the multilayer. We can associate the presence of water to the uncompensated charges present in the outermost region of the film. To elucidate the chemical nature of the outermost layers we performed XPS and zeta potential characterization of multilayers grown under different assembly conditions.

Table 2 shows the chemical composition of (PSS-MA/PDADMAC)$_{10}$ multilayers. XPS analyze approximately the top 10 nm of the sample.[68] In general, the thickness of one layer is less than 10 nm, thus the results obtained contain information from more than one assembled layer.

Sulfur atoms are only present in PSS-MA while nitrogen is only present in PDADMAC. As expected, S content was higher for the films with PSS-MA capping layers in comparison with the values associated to those with PDADMAC capping layers. In the same way, after PDADMAC deposition greater quantities of N were detected. But, by and large, it can be said that the S : N ratio is close to 1 within the topmost region ($\sim$10 nm) of the multilayers or, in other words, the outer region of the film contains an equimolar amount of quaternary amines and sulfonate groups. On the other hand, in the case of multilayers grown under saline conditions the presence of potassium and chloride can be detected. Note that the amount of K^+ is always

 This journal is © the Owner Societies 2015

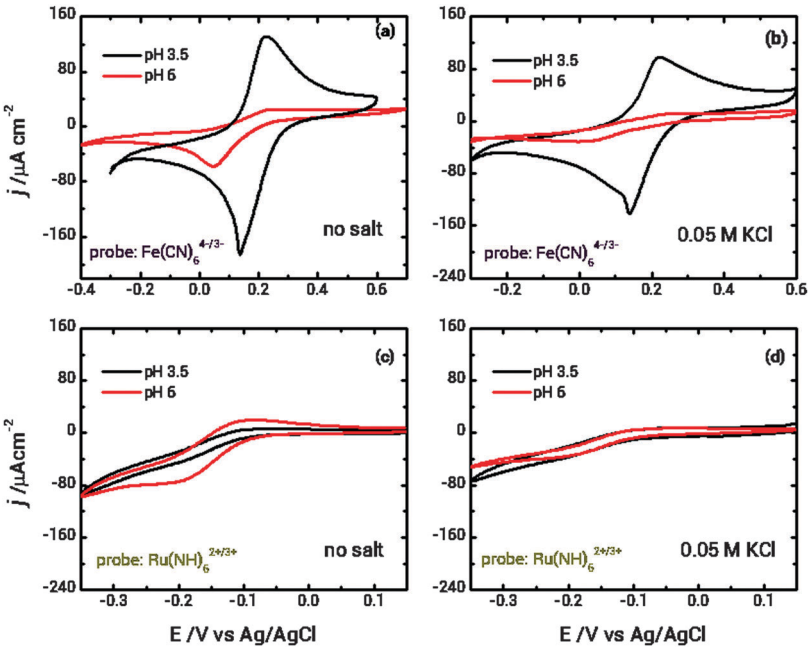

Fig. 3 Cyclic voltammograms corresponding to Au electrodes coated with PDADMAC-capped $(PSS\text{-}MA/PDADMAC)_{10}$ multilayers assembled in pure water (a) and in 0.05 M KCl (b) in the presence of the anionic probes $Fe(CN)_6^{3-/4-}$ and similar multilayers assembled in pure water (c) and in 0.05 M KCl (d) in the presence of the cationic probes $Ru(NH_3)_6^{2+/3+}$. Scan rate: 10 mV s^{-1}.

Table 2 Atomic fraction from XPS analysis of films of $(PSS\text{-}MA/PDADMAC)_9/PSS\text{-}MA$ and $(PSS\text{-}MA/PDADMAC)_9/PSS\text{-}MA/PDADMAC$

		Atom%					
pH	Capping layer	[KCl]	S	N	Cl	K	S/N
3.5	PSS-MA	None	4.4	3.0	—	—	1.46
	PDADMAC	None	3.7	4.6	—	—	0.80
	PSS-MA	0.2 M	3.7	4.2	1.0	3.2	0.88
	PDADMAC	0.2 M	3.0	4.6	2.7	4.8	0.65
6	PSS-MA	None	4.5	2.6	0.5	—	1.73
	PDADMAC	None	3.8	3.8	1.0	—	1.00
	PSS-MA	0.2 M	4.4	4.0	0.4	3.4	1.10
	PDADMAC	0.2 M	3.5	4.5	1.8	1.5	0.78
9.5	PSS-MA	None	4.7	5.6	1.0	—	0.84
	PDADMAC	None	2.4	7.6	2.1	—	3.16
	PSS-MA	0.2 M	4.6	4.3	1.1	4.8	1.07
	PDADMAC	0.2 M	4.2	4.1	2.5	8.5	1.02

larger than that of Cl^- regardless of the polyelectrolyte in the capping layer. If we consider that the "extrinsic compensation" mechanism operates in the whole assembly, then the excess amount of K^+ ions with respect to Cl^- hints for the presence of ionized carboxylate units remaining "silently" in the multilayer. We use the term "silent" to denote that even though carboxylate groups are charged they do not play an active role in the purely electrostatic assembly of the multilayer. This can be inferred from the fact that there are comparable amounts of sulfonate and carboxylate groups on each polyanion chain ($SO_3^-:COO^-$ is 3 : 2) but XPS analysis indicated that quaternary amines and sulfonate groups are present in nearly equimolar amounts ($SO_3^-:QA^+ \sim 1$). This suggests that there are fixed negative charges that do not form ion pairs with the corresponding counterpolyelectrolyte and might be "activated" by changes in the environmental pH. This surmise was tested measuring the zeta potential of $(PSS\text{-}MA/PDADMAC)_{10}$ multilayers prepared under different assembly conditions. As can be seen in Table 2 at pH 3.5, an experimental condition where carboxylate units are "turned-off", the sign of the ζ potential is defined by the type of polyelectrolyte in the capping layer, *i.e.* PDADMAC leads to positive ζ potential values whereas PSS-MA leads to negative ζ potential values. This observation is in full agreement with the so-called "charge reversal" mechanism operating during the multilayer build up.

Interestingly, at pH 6 we observed that charge reversal operated in assemblies prepared in pure water, but no longer operated in multilayers grown under saline conditions. This effect is even more pronounced at pH 9.5, where the presence of PDADMAC as the capping layer cannot reverse the negative ζ potential of the multilayer. This can be interpreted considering the rich interplay between molecular organization, interactions and chemical equilibrium, which ultimately leads to a non-trivial coupling of design variables. Increasing pH levels from 3.5 to 6 implies the generation of negative charges within the film due to the ionization of "silent" carboxylate groups. In the case of samples prepared under saline conditions the interdiffusion of polyelectrolyte layers in the outer region of the multilayer leads to a situation in which fixed negative charges in excess are strongly interdigitated with fixed positive charges in defect, with the concomitant result of negative ζ potential values. Then, when the pH was further increased to 9.5 the effect of the "silent" ionized carboxylate groups played an even more dominant role and the manifestation of more negative ζ potential values was observed in all the samples, including

those assembled in pure water and presenting PDADMAC as the capping layer (see Table 3). Regarding the latter, we should note that according to detailed studies reported by Donath *et al.*[69] not only the capping layer but also the underneath layers contribute to the ζ potential. Hence, even though samples prepared in pure water may exhibit low levels of interdigitation, the pH-induced appearance of fixed negative charges underneath the outermost PDADMAC layer is sufficient to control the magnitude and sign of the ζ potential.

Within this context, it is important to highlight that several LbL assemblies displaying pH-responsive properties have been reported. Despite these burgeoning achievements, many of the existing pH-responsive LbL systems have disadvantages such as the profound structural reorganization and limited stability of multilayers in saline environments. In particular, Rubner and co-workers showed that pH-induced phase separation of PAA–PAH yields highly porous films.[70] Concomitantly, Sui and Schlenoff reported that multilayers containing weak polyelectrolytes evidence pH-induced cratering in the surface morphology.[71] Contrarily, systems comprising weak–strong copolymer polyelectrolyte multilayers showed no evidence of cratering or phase-separation during pH switching from acidic to alkaline conditions. In addition, it has been demonstrated that too many counterion-compensated units within a multilayer cause hyperswelling and decomposition.[72,73] This phenomenology is highly plausible and reasonable due to the fact that pH-tunable electrostatic interactions between oppositely charged polyelectrolytes play a structural role within the assembly.

However, this is not the case of multilayers assembled in the presence of "silent" charges given that it has been demonstrated that carboxylate groups do not interact with PDADMAC and consequently the chemical equilibrium of the embedded weak anionic groups does not compromise the multilayer stability. In this particular setting the structural role is exclusively played by quaternary ammonium ions and sulfonate groups that are responsible for stitching together the multilayer at all pH values. These "silent" charges can be exploited to tailor not only the pH-responsive properties of the film but also to further control its ion transport properties. With this background in mind and being aware of the interesting properties of our system we electrochemically probed the pH-tunable permeability of anionic redox active probes, $Fe(CN)_6^{4-}$ and $Fe(CN)_6^{3-}$ ions, diffusing through PSS-MA/PDADMAC multilayers grown on gold electrodes using cyclic voltammetry. We prepared gold electrodes modified with $(PSS\text{-}MA/PDADMAC)_{10}$ films assembled under different pH and ionic strength conditions, and their cyclic voltammograms (CVs) were measured in a 1 mM $Fe(CN)_6^{3-}$ + 1 mM $Fe(CN)_6^{4-}$ solution and a 1 mM $Ru(NH_3)_6^{2+}$ + 1 mM $Ru(NH_3)_6^{3+}$ solution, respectively, both containing 0.1 M KCl as a supporting electrolyte. Fig. 3 shows CVs of the redox probes on the Au electrodes coated with PDADMAC-capped $(PSS\text{-}MA/PDADMAC)_{10}$ multilayers prepared in pure water. CVs were recorded after the electrodes had been immersed in the solution containing the redox probes for *ca.* 20 min because the magnitude of the electrochemical signal increased with time during the first minutes.

Measurements performed at pH 3.5 displayed a well-defined voltammetric response which was indicative of redox probes diffusing through the film. However, for similar measurements performed at pH 6, the redox response of the electroactive ions was severely suppressed. The sharp decrease in the electrochemical signal originates from the exclusion of the redox-active anions from the multilayer. As hypothesized, this exclusion process stems from the pH-induced generation of excess negative charges within the film. PSS-MA/PDADMAC multilayers were characterized by FTIR to corroborate the ionization of the carboxylic acid groups within the film (Fig. 4). The peak at 1720 cm^{-1} stems from the C=O stretching of COOH groups whereas peaks at 1580 and 1412 cm^{-1} are due to asymmetric and symmetric stretching of COO^- moieties. Peaks observed in the 1250–1000 cm^{-1} range are due to the presence of sulfonate groups. For PSS-MA/PDADMAC multilayers at pH 3.5 almost all the carboxylic acid groups are protonated as indicated by the presence of the COOH peak at 1720 cm^{-1} and the absence of COO^- signal at 1412 cm^{-1}. Upon increasing pH, the intensity of the COOH band is more tenuous, while the intensities of the COO^- bands at 1580 and 1412 cm^{-1} notoriously increase. Consequently, FTIR characterization conclusively confirms a marked increase in the number of ionized acid groups within the multilayer when pH is increased from 3.5 to 6.

Table 3 ζ potential of $(PDADMAC/PSS\text{-}MA)_4$/PDADMAC and $(PDADMAC/PSS\text{-}MA)_4$/PDADMAC/PSS-MA multilayers

		ζ potential/mV		
pH	Capping layer	No KCl	0.05 M KCl	0.2 M KCl
3.5	PSS-MA	−40.1	−49.4	−50.3
	PDADMAC	74.5	60.5	57.6
6	PSS-MA	−33.6	−40.2	−20.5
	PDADMAC	27.5	−18.1	−15.2
9.5	PSS-MA	−55.2	−48	−47.7
	PDADMAC	−61.4	−52.1	−52.3

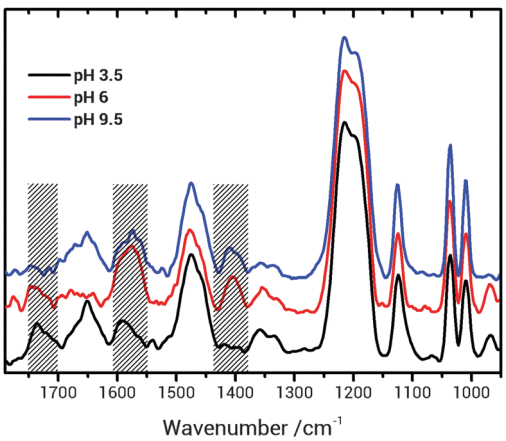

Fig. 4 FTIR spectra of $(PSS\text{-}MA/PDADMAC)_9$/PDADMAC multilayers previously immersed in 0.1 M KCl at different pH values: pH 3.5 (black trace), pH 6 (red trace) and pH 9.5 (blue trace).

 This journal is © the Owner Societies 2015

Note that in the electrochemical experiments of permselectivity the capping layer is PDADMAC that, in principle, would attract the anionic probes to the film. However, the extent of fixed negative charges generated within the film by increasing the pH from 3.5 to 6 completely precludes the passage of anions through the multilayer due to strong electrostatic repulsions. A similar result has been observed for multilayers grown under different saline conditions, indicating that in the case of PSS-MA/PDADMAC multilayers their pH-regulated ion-gating properties are not affected when films are grown in an exponential fashion involving considerable uptake of solvent and ions. Concomitantly, the strong cationic nature of the PDADMAC capping layer plays a role as a "permanent gatekeeper" precluding the passage of cationic probes at all pH values due to electrostatic repulsion. In this regard, Calvo and Wolosiuk[74] demonstrated that in electroactive polyelectrolyte multilayers, the charge of the capping layer itself may play an important role in regulating the permselective properties of the multilayer. As a result, in our experimental setting the combination of pH-responsive "silent" charges embedded into the film and a strong cationic layer sitting atop the film permits the creation of an anion-selective, proton-gated interfacial architecture that acts as a gateable ionic filter enabling the selective passage of anions only under determined pH conditions, whereas the passage of cations is repelled regardless of the proton concentration (Scheme 1). This interesting behavior in which the interface displays ion-selective pH-activated gating properties (*i.e.*: rectified ion transport) resembles that observed in acid-sensing ion channels (ASICs) in peripheral sensory neurons and in the neurons of the central nervous system, in which the biological pore exerts active control over the flow of cations and fully precludes the transport of anions.[75]

Within this context we should consider that, even though the multilayer constitutes of strong- and weak acid repeat units, the presence of weak acids often causes irreversible morphology changes that could affect the ion transport properties. To this end, we performed *in situ* AFM imaging during pH cycling. Fig. 5 displays the significant morphological changes undergone by the film after cyclic exposure to solutions with pH = 6 and 3.5. These observations confirm the pH-induced structural reorganization taking place during the pH cycling that ultimately leads to the formation of small pores (see green arrows in Fig. 5). We then confirmed through cyclic voltammetric experiments that this film reorganization had a strong impact on the ion transport properties and/or permeability of the multilayer. Cyclic voltammograms of PSS-MA/PDADMAC multilayers in the presence of $Fe(CN)_6^{3-/4-}$ and $Ru(NH_3)_6^{2+/3+}$ after extensive pH cycling showed that the permselective transport properties in the presence of anionic probes were no longer operating whereas the gatekeeping effect was only observed in the case of the cationic probes (Fig. 6). In other words, voltammetric experiments showed that after extensive pH cycling multilayers are highly permeable to $Fe(CN)_6^{3-/4-}$ and impermeable to $Ru(NH_3)_6^{2+/3+}$ probes. This indicates that, despite the fact that pH cycling does no affect the integrity of the multilayers, film reorganization strongly affects their permselective properties probably due to the formation of pores that at last generate pathways for the transport of charged probes. We hypothesize

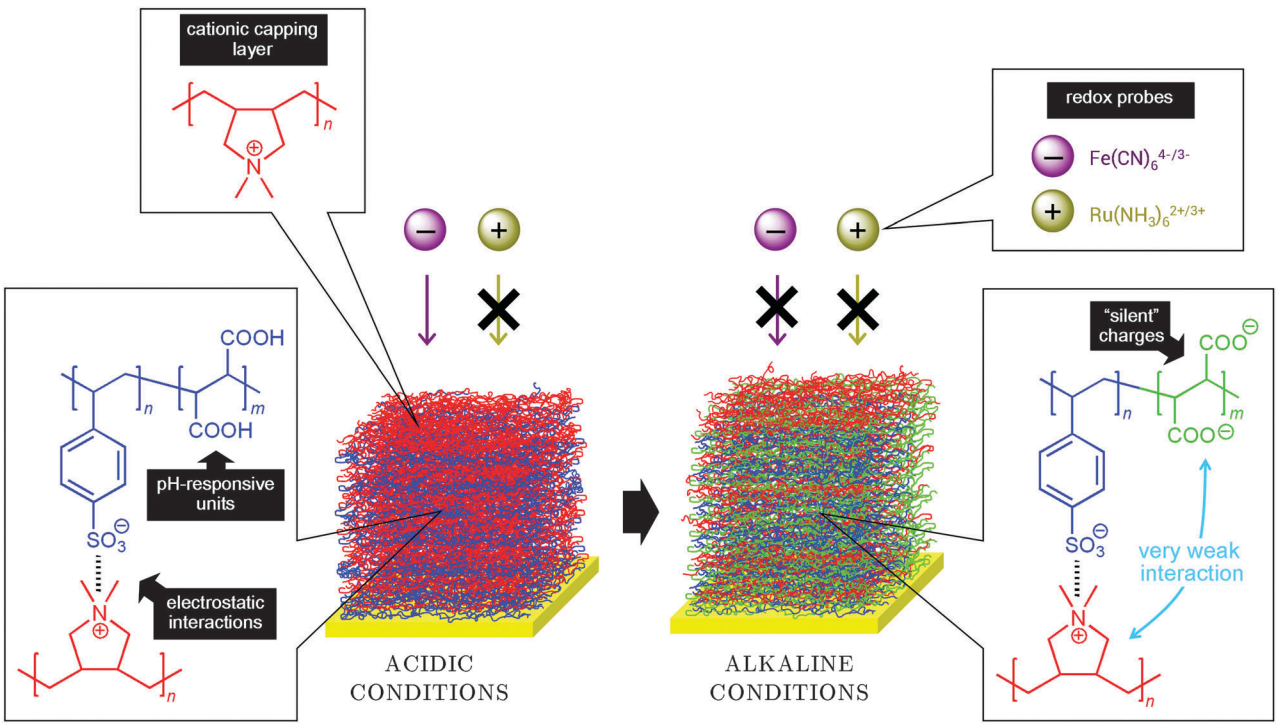

Scheme 1 Schematic illustration of the pH-switchable function of the multilayered thin film. At high pH the film has a net negative charge resulting from the ionization "silent" carboxyl groups embedded in the film during the electrostatic assembly that precludes the passage of anions.

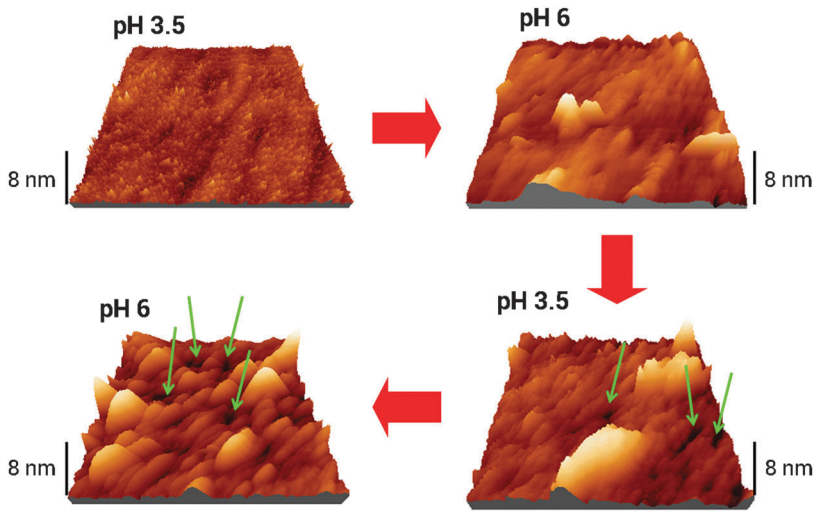

Fig. 5 *In situ* atomic force microscopy imaging (5 × 5 μm^2) of (PSS-MA/PDADMAC)$_{10}$ multilayers assembled in pure water at pH 3.5 and subjected to cyclic pH changes (between pH 3.5 and 6).

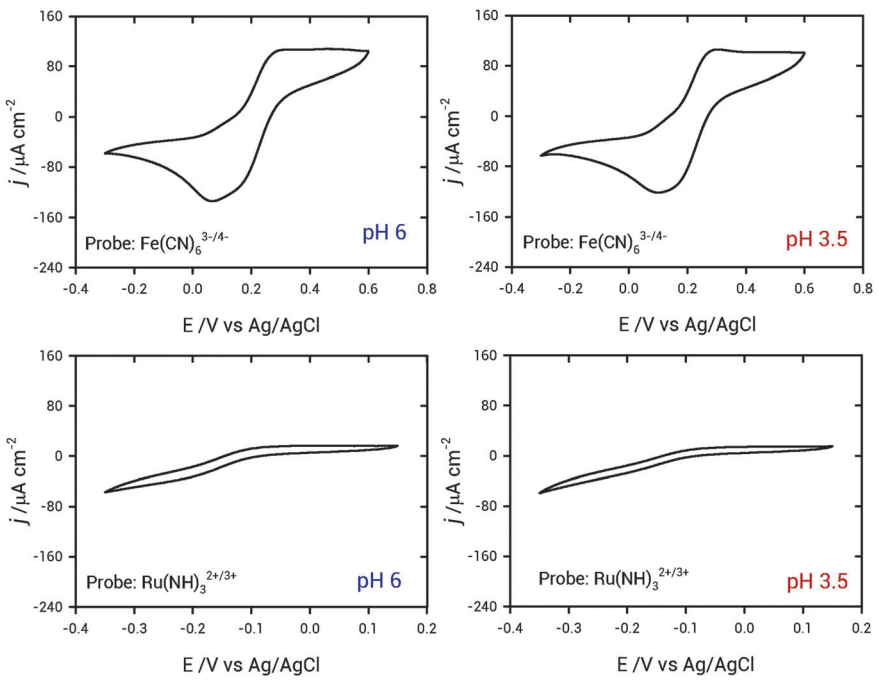

Fig. 6 Cyclic voltammograms of anionic and cationic redox probes in contact with Au electrodes coated with PDADMAC-capped (PSS-MA/PDADMAC)$_{10}$ multilayers after extensive pH cycling between pH 6 and 3.5. Scan rate: 10 mV s^{-1}.

that the gatekeeping effect is due to the presence of PDADMAC in the outermost layer of the film that, in spite of reorganization, still precludes the diffusion of $Ru(NH_3)_6^{2+/3+}$ probes due to repulsive electrostatic interactions.

Conclusions

An understanding of the supramolecular growth of PSS-MA/PDADMAC multilayers under different assembly conditions led to the design and preparation of functional interfacial architectures displaying interesting pH-controlled ion-gating properties. Aided by previous studies, characterization of PSS-MA/PDADMAC multilayers through a multitechnique approach provided a more in-depth understanding of the delicate interplay between molecular organization, inter-polyelectrolyte interactions and chemical equilibrium taking place during the assembly and exposure of these assemblies to solutions of different pH values and ionic strengths. We showed for the first time the use of weak–strong anionic polyelectrolytes as building blocks that can interact differentially with the cationic counter-polyelectrolyte to confer ion-gating properties to the multilayered thin film. These surface-confined architectures are very stable under

 This journal is © the Owner Societies 2015

different pH and saline conditions and operate as supramolecular gates as a function of pH: at low pH anions can easily penetrate, while at high pH they are excluded from the film. The switching behavior of these multilayer films was attributed to the presence of ionizable carboxylate groups that do not participate in the electrostatic assembly due to poor interaction with the polycation, but remain "silent" within the film and play an active role when the pH of the solution is increased, without compromising the structural stability of the multilayer. When these interesting properties are combined with a strong cationic capping layer that repels the passage of cationic probes, a pH-active rectified transport of anions is observed. Herein, however, it must be considered that these interesting functional properties can be significantly affected when multilayers are subjected to extensive pH cycling as a result of irreversible morphological changes leading to the formation of holes in the film structure, as observed by *in situ* AFM imaging. Nevertheless, we should note that this film reorganization does not compromise the structural integrity of the multilayer.

Considering the versatile nature of layer-by-layer assembly these proof-of-principle experiments using poly(4-styrenesulfonic acid-*co*-maleic acid) could be easily extended to other weak–strong polyelectrolyte systems displaying contrasting ion-pairing interactions with the corresponding polycations. These results introduce an interesting example of molecular design of multilayer assemblies whose structural integrity is given exclusively by noncovalent interactions, in which inter-polyelectrolyte electrostatic binding stabilizes the structure while "silent" weak polyelectrolyte units mediate the pH-responsive function of the whole assembly. Bearing in mind these results, we envision that this study will offer opportunities and insights for further development of the blossoming discipline known as "nanoarchitectonics",[76] as well as for the construction of soft interfaces displaying switchable transport properties.[77]

Experimental section

Materials

Poly(4-styrenesulfonic acid-*co*-maleic acid), sodium salt (PSS-MA; M_w 20.000 g mol^{-1}; 3 : 1 SS : MA), poly(diallyldimethylammonium chloride) solution 20% in H_2O (PDADMAC; average $M_w \sim$ 100.000–200.000 g mol^{-1}), polyethylenimine (PEI, $M_w \sim$ 25 000 g mol^{-1}), hexaammineruthenium(II) chloride and hexaammineruthenium(III) chloride were purchased from Sigma-Aldrich. Boric acid, acetic acid and sodium acetate from Anedra and sodium hydroxide from Biopack were used for buffer solutions. Potassium hexacyanoferrate(III) and potassium chloride were acquired from Anedra and potassium hexacyanoferrate(II) trihydrate was purchased from Biopack.

All chemicals were used without further purification. Ultrapure water (Milli-Q) with a resistivity of 18 MΩ cm was used in all experiments. Experiments were carried out at room temperature.

Preparation of multilayer films

The polymer deposition solutions were prepared with buffers at pH 3.5, 6 and 9.5. The pH was adjusted in both polymer solutions in order to avoid the change of the pH exposure of PSS-MA during the PDADMAC assembly process. The ionic strength was adjusted using no salt addition, 0.05 M and 0.2 M KCl.

The Au substrates were first coated with PEI (1 mg mL^{-1}) for 15 min and then rinsed with Milli-Q water. Multilayer films were assembled by the sequential process, alternating between PSS-MA solution (1 mg mL^{-1}) and PDADMAC solution (1 mg mL^{-1}). The substrates were rinsed with Milli-Q water after each adsorption step. Ten bilayers, (PSS-MA/PDADMAC)$_{10}$, were assembled.

Surface plasmon resonance

SPR detection was carried out using an SPR-Navi 210A setup (BioNavis Ltd, Tampere, Finland) using gold sensor slides provided by Bionavis. Thickness calculation was performed using the "Winspall" software employing $n = 1.48$ as the refractive index for both PSS-MA and PDADMAC polyelectrolytes. The surface coverage (Γ) was determined from Freijter's equation,[78] which can be expressed as

$$\Gamma = \frac{\Delta\theta k d}{\mathrm{d}n/\mathrm{d}c}$$

where θ is the angular response in the measurement, k the instrument constant, d the sample layer thickness and dn/dc the dependency of the refraction index concentration. For the calculation, $k \times d = 1.9 \times 10^{-7}$ cm deg^{-1} and dn/dc = 0.197 cm^3 g^{-1} were used for λ = 785 nm.

Quartz crystal microbalance with dissipation monitoring

The QCM-D measurements were carried out using a Q-Sense E4 quartz crystal microbalance (Q-Sense, Göteborg, Sweden) using Au (50 nm)-coated quartz crystals (5 MHz) (QSX-301, Q-Sense) previously treated with a UV-Ozone cleaning protocol. For films considered rigid enough, it is possible to calculate the areal mass from QCM-D data using the Sauerbrey equation[79]

$$\Delta m = -\frac{C\Delta f}{n}$$

where Δf is the change in frequency, Δm the change in mass, n the overtone number and C the mass sensitivity constant.

Electrochemical measurements

Cyclic voltammetry experiments were performed using a potentiostat TEQ-04 and a conventional three electrode cell equipped with a Ag/AgCl reference electrode and a platinum counter electrode. The electrochemical experiments were performed in the PDADMAC-capped (PSS-MA/PDADMAC)$_{10}$ multilayers. Cyclic voltammograms of potassium ferrocyanide/potassium ferricyanide ($[Fe(CN)_6]^{4-/3-}$) 1 × 10^{-3} M solutions + 0.1 M KCl and hexaammineruthenium(II) chloride/hexaammineruthenium(III) chloride ($[Ru(NH_3)_6]^{2+/3+}$) 1 × 10^{-3} M solutions + 0.1 M KCl were registered, respectively. The pH of $[Fe(CN)_6]^{4-/3-}$ and $Ru(NH_3)_6^{2+/3+}$ solutions was the same as the polyelectrolyte solutions used in the film construction.

Dynamic light scattering

The ζ potential of layer by layer assembly was measured by DLS. The measurements were performed using a Malvern Zetasizer Nano ZS at a scattering angle of 173° at 25 °C with a He–Ne 633 nm laser. The layer by layer assemblies were prepared on SiO_2 particles at pH 3.5, 6 and 9.5 and the ionic strength was adjusted without salt addition and with 0.05 and 0.2 M KCl at each pH. The measurements were performed at the same pH of assembly. The SiO_2 particles were synthesized as described by Stober and Fink.[80]

Atomic force microscopy

The films were imaged in the contact mode in air and in the tapping mode in liquid at room temperature with a Multimode AFM (Veeco) connected to a Nanoscope V controller. Non-conductive silicon nitride cantilevers (Bruker) with a K = 0.35 N m^{-1} were used.

X-Ray photoelectron spectroscopy

XPS experiments were performed on a SPECS Sage HR 100 spectrometer with a non-monochromatic X-ray source (Mg Kα line of 1253.6 eV). All measurements were done on an ultra-high vacuum (UHV) chamber at a pressure of about 5×10^{-8} mbar. Gaussian–Lorentzian functions were used to perform the curve fitting of the high resolution spectra.

FTIR spectroscopy

Fourier transform infrared spectroscopy in the attenuated total reflection mode (ATR-FTIR) was performed using a Varian 600 FTIR spectrometer equipped with a ZnSe ATR crystal with a resolution of 1 cm^{-1}. Background-subtracted spectra were corrected for ATR acquisition.

Acknowledgements

The authors acknowledge financial support from ANPCyT (PICT 2010-2554, PICT-2013-0905 and PPL 2011-003), Fundación Petruzza and the Austrian Institute of Technology GmbH (AIT–CONICET Partner Lab: *"Exploratory Research for Advanced Technologies in Supramolecular Materials Science"* – Exp. 4947/11, Res. No. 3911, 28-12-2011). E.M. and J.S.T acknowledge CONICET for their postdoctoral fellowships. O.A. is a CONICET fellow.

References

1 R. K. Iler, *J. Colloid Interface Sci.*, 1966, **21**, 569–594.
2 G. Decher and J.-D. Hong, *Ber. Bunsenges. Phys. Chem.*, 1991, **95**, 1430–1434.
3 (*a*) M. Coustet, J. Irigoyen, T. Alonso Garcia, R. A. Murray, G. Romero, M. S. Cortizo, W. Knoll, O. Azzaroni and S. E. Moya, *J. Colloid Interface Sci.*, 2014, **421**, 132–140; (*b*) M. L. Cortez, N. De Matteis, M. Ceolín, W. Knoll, F. Battaglini and O. Azzaroni, *Phys. Chem. Chem. Phys.*, 2014, **16**, 20844–20855; (*c*) D. Pallarola, C. von Bildering, L. I. Pietrasanta, N. Queralto, W. Knoll. F. Battaglini and O. Azzaroni, *Phys. Chem. Chem. Phys.*, 2012, **14**, 11027–11039; (*d*) O. Azzaroni and K. H. A. Lau, *Soft Matter*, 2011, **7**, 8709–8724; (*e*) M. Ali, B. Yameen, J. Cervera, P. Ramírez, R. Neumann, W. Ensinger, W. Knoll and O. Azzaroni, *J. Am. Chem. Soc.*, 2010, **132**, 8338–8348; (*f*) D. Pallarola, N. Queralto, F. Battaglini and O. Azzaroni, *Phys. Chem. Chem. Phys.*, 2010, **12**, 8071–8083; (*g*) J. Irigoyen, S. E. Moya, J. J. Iturri, I. Llarena, O. Azzaroni and E. Donath, *Langmuir*, 2009, **25**, 3374–3380.
4 (*a*) K. Ariga, Q. Ji, J. P. Hill, Y. Bando and M. Aono, *NPG Asia Mater.*, 2012, **4**, e17; (*b*) K. Ariga, Q. Ji and J. P. Hill, *Adv. Polym. Sci.*, 2010, **229**, 51–87; (*c*) K. Ariga, J. P. Hill and Q. Ji, *Phys. Chem. Chem. Phys.*, 2007, **9**, 2319–2340; (*d*) K. Ariga, Y. Yamauchi, G. Rydzek, Q. Ji, Y. Yonamine, K. C.-W. Wu and J. P. Hill, *Chem. Lett.*, 2014, **43**, 36–68.
5 (*a*) D. Volodkin, A. Skirtach and H. Möhwald, *Bioactive Surf.*, 2011, **240**, 135–161; (*b*) P. Bertrand, A. Jonas, A. Laschewsky and R. Legras, *Macromol. Rapid Commun.*, 2000, **21**, 319–348; (*c*) Y. Ma, W.-F. Dong, M. A. Hempenius, H. Möhwald and G. J. Vancso, *Angew. Chem., Int. Ed.*, 2007, **46**, 1702–1705; (*d*) A. G. Skirtach, P. Karageorgiev, M. F. Bédard, G. B. Sukhorukov and H. Möhwald, *J. Am. Chem. Soc.*, 2008, **130**, 11572–11573; (*e*) G. Sukhorukov, A. Fery and H. Möhwald, *Prog. Polym. Sci.*, 2005, **30**, 885–897.
6 M. Eckle and G. Decher, *Nano Lett.*, 2001, **1**, 45–49.
7 J. Hiller, J. D. Mendelsohn and M. F. Rubner, *Nat. Mater.*, 2002, **1**, 59–63.
8 X. Liu and M. L. Bruening, *Chem. Mater.*, 2004, **16**, 351–357.
9 Z. Tang, N. A. Kotov, S. Magonov and B. Ozturk, *Nat. Mater.*, 2003, **2**, 413–418.
10 T. Farhat and P. T. Hammond, *Adv. Funct. Mater.*, 2005, **15**, 945–954.
11 E. Vazquez, D. M. Dewitt, P. T. Hammond and D. M. Lynn, *J. Am. Chem. Soc.*, 2002, **124**, 13992–13993.
12 R. M. Flessner, Y. Yu and D. M. Lynn, *Chem. Commun.*, 2011, **47**, 550–552.
13 N. Jessel, F. Atalar, P. Lavalle, J. Mutterer, G. Decher, P. Schaaf, J.-C. Voegel and J. Ogier, *Adv. Mater.*, 2003, **15**, 692–695.
14 N. S. Zacharia, M. Modestino and P. T. Hammond, *Macromolecules*, 2007, **40**, 9523–9528.
15 K. Itano, J. Choi and M. F. Rubner, *Macromolecules*, 2005, **38**, 3450–3460.
16 S. Biggs and A. D. Proud, *Langmuir*, 1997, **13**, 7202–7210.
17 S. T. Dubas and J. B. Schlenoff, *Macromolecules*, 2001, **34**, 3736–3740.
18 Z. Sui, D. Salloum and J. B. Schlenoff, *Langmuir*, 2003, **19**, 2491–2495.
19 N. S. Zacharia, D. M. De Longchamp, M. Modestino and P. T. Hammond, *Macromolecules*, 2007, **40**, 1598–1603.
20 E. Tjipto, J. F. Quinn and F. Caruso, *J. Polym. Sci., Part A: Polym. Chem.*, 2007, **45**, 4341–4351.
21 G. Liu, J. Zhao, Q. Sun and G. Zhang, *J. Phys. Chem. B*, 2008, **112**, 3333–3338.
22 C. C. Buron, C. Filiâtre, F. Membreya, C. Bainier, D. Charraut and A. Foissy, *J. Colloid Interface Sci.*, 2007, **314**, 358–366.

 This journal is © the Owner Societies 2015

23 X. Gong and C. Gao, *Phys. Chem. Chem. Phys.*, 2009, **11**, 11577–11586.
24 G. Liu, Y. Hou, X. Xiao and G. Zhang, *J. Phys. Chem. B*, 2010, **114**, 9987–9993.
25 R. A. Ghostine, M. Z. Markarian and J. B. Schlenoff, *J. Am. Chem. Soc.*, 2013, **135**, 7636–7646.
26 Y. Ma, J. Dong, S. Bhattacharjee, S. Wijeratne, M. L. Bruening and G. L. Baker, *Langmuir*, 2013, **29**, 2946–2954.
27 D. Yoo, S. S. Shiratori and M. F. Rubner, *Macromolecules*, 1998, **31**, 4309–4318.
28 S. S. Shiratori and M. F. Rubner, *Macromolecules*, 2000, **33**, 4213–4219.
29 S. M. Notley, M. Eriksson and L. Wågberg, *J. Colloid Interface Sci.*, 2005, **292**, 29–37.
30 J. Fu, J. Ji, L. Shen, A. Küller, A. Rosenhahn, J. Shen and M. Grunze, *Langmuir*, 2009, **25**, 672–675.
31 P. Bieker and M. Schönhoff, *Macromolecules*, 2010, **43**, 5052–5059.
32 N. Fujii, K. Fujimoto, T. Michinobu, M. Akada, J. P. Hill, S. Shiratori, K. Ariga and K. Shigehara, *Macromolecules*, 2010, **43**, 3947–3955.
33 J. D. Mendelsohn, C. J. Barrett, V. V. Chan, A. J. Pal, A. M. Mayes and M. F. Rubner, *Langmuir*, 2000, **16**, 5017–5023.
34 T. Alonso, J. Irigoyen, J. J. Iturri, I. L. Larena and S. E. Moya, *Soft Matter*, 2013, **9**, 1920–1928.
35 (*a*) L. Krasemann, A. Toutianoush and B. Tieke, *J. Membr. Sci.*, 2001, **181**, 221–228; (*b*) A. M. Balachandra, J. H. Dai and M. L. Bruening, *Macromolecules*, 2002, **35**, 3171–3178.
36 S. Han and B. Lindholm-Sethson, *Electrochim. Acta*, 1999, **45**, 845–853.
37 (*a*) T. R. Farhat and J. B. Schlenoff, *Langmuir*, 2001, **17**, 1184–1192; (*b*) V. Pardo-Yissar, E. Katz, O. Lioubashevski and I. Willner, *Langmuir*, 2001, **17**, 1110–1118.
38 T. R. Farhat and J. B. Schlenoff, *J. Am. Chem. Soc.*, 2003, **125**, 4627–4636.
39 T. R. Farhat and J. B. Schlenoff, *Electrochem. Solid-State Lett.*, 2002, **5**, B13–B15.
40 (*a*) Y. L. Liu, M. Q. Zhao, D. E. Bergbreiter and R. M. Crooks, *J. Am. Chem. Soc.*, 1997, **119**, 8720–8721; (*b*) S. E. Burke and C. J. Barrett, *Macromolecules*, 2004, **37**, 5375–5384.
41 M. K. Park, S. Deng and R. C. Advincula, *J. Am. Chem. Soc.*, 2004, **126**, 13723–13731.
42 (*a*) G. Wu, F. Shi, Z. Wang, Z. Liu and X. Zhang, *Langmuir*, 2009, **25**, 2949–2955; (*b*) H. Chen, G. Zeng, Z. Wang and X. Zhang, *Macromolecules*, 2007, **40**, 653–660.
43 (*a*) Y. F. Cheng, L. Murtomaki and R. M. Corn, *J. Electroanal. Chem.*, 2000, **483**, 88–94; (*b*) T. Noguchi and J. Anzai, *Langmuir*, 2006, **22**, 2870–2875.
44 E. Tjipto, J. F. Quinn and F. Caruso, *Langmuir*, 2005, **21**, 8785–8792.
45 X. Gong, *Phys. Chem. Chem. Phys.*, 2013, **15**, 10459–10465.
46 F. Boulmedais, V. Ball, P. Schwinte, B. Frisch, P. Schaaf and J.-C. Voegel, *Langmuir*, 2003, **19**, 440–445.
47 P. Lavalle, C. Picart, J. Mutterer, C. Gergely, H. Reiss, J.-C. Voegel, B. Senger and P. Schaaf, *J. Phys. Chem. B*, 2004, **108**, 635–648.
48 C. Porcel, P. Lavalle, V. Ball, G. Decher, B. Senger, J.-C. Voegel and P. Schaaf, *Langmuir*, 2006, **22**, 4376–4383.
49 C. Porcel, P. Lavalle, G. Decher, B. Senger, J.-C. Voegel and P. Schaaf, *Langmuir*, 2007, **23**, 1898–1904.
50 O. Svensson and T. Arnebrant, *Curr. Opin. Colloid Interface Sci.*, 2010, **15**, 395–405.
51 L. Xu, D. Pristinski, A. Zhuk, C. Stoddart, J. F. Ankner and S. A. Sukhishvili, *Macromolecules*, 2012, **45**, 3892–3901.
52 C. Peng, Y. S. Thio, R. A. Gerhardt, H. Ambaye and V. Lauter, *Chem. Mater.*, 2011, **23**, 4548–4556.
53 (*a*) P. Bieker and M. Schönhoff, *Macromolecules*, 2010, **43**, 5052–5059; (*b*) J. Fu, J. Ji, L. Shen, A. Ku, A. Rosenhahn, J. Shen and M. Grunze, *Langmuir*, 2009, 672–675; (*c*) L. Xu, D. Pristinski, A. Zhuk, C. Stoddart, J. F. Ankner and S. A. Sukhishvili, *Macromolecules*, 2012, **45**, 3892–3901.
54 H. Mjahed, G. Cado, F. Boulmedais, B. Senger, P. Schaaf, V. Ball and J.-C. Voegel, *J. Mater. Chem.*, 2011, **21**, 8416.
55 X. Gong, L. Han, Y. Yue, J. Gao and C. Gao, *J. Colloid Interface Sci.*, 2011, **355**, 368–373.
56 M. K. Park and R. Advincula, in *Functional Polymer Films*, ed. W. Knoll and R. C. Advincula, VCH-Wiley, Weinheim, 2011.
57 H. W. Jomaa and J. B. Schlenoff, *Macromolecules*, 2005, **38**, 8473–8480.
58 N. S. Zacharia, M. Modestino and P. T. Hammond, *Macromolecules*, 2007, **40**, 9523–9528.
59 J. Chen, L. Dumas, J. Duchet-Rumeau, E. Fleury, A. Charlot and D. Portinha, *J. Polym. Sci., Part A: Polym. Chem.*, 2012, **50**, 3452–3460.
60 A. I. Petrov, A. A. Antipov and G. B. Sukhorukov, *Macromolecules*, 2003, **36**, 10079–10086.
61 (*a*) M. Schönhoff, V. Ball, A. R. Bausch, C. Dejugnat, N. Delorme, K. Glinel, R. von Klitzing and R. Steitz, *Colloids Surf., A*, 2007, **303**, 14–29; (*b*) J. B. Schlenoff, A. H. Rmaile and C. B. Bucur, *J. Am. Chem. Soc.*, 2008, **130**, 13589–13597.
62 M. Schönhoff, V. Ball, A. R. Bausch, C. Dejugnat, N. Delorme, K. Glinel, R. V. Klitzing and R. Steitz, *Colloids Surf., A*, 2007, **303**, 14–29.
63 (*a*) S. M. Notley, M. Eriksson and L. Wagberg, *J. Colloid Interface Sci.*, 2005, **292**, 29–37; (*b*) J. J. Iturri Ramos, I. Llarena, L. Fernandez, S. E. Moya and E. Donath, *Macromol. Rapid Commun.*, 2009, **30**, 1756–1761.
64 (*a*) P. Lavalle, C. Gergely, F. J. G. Cuisinier, G. Decher, P. Schaaf, J.-C. Voegel and C. Picart, *Macromolecules*, 2002, **35**, 4458–4465; (*b*) L. A. Connal, Q. Li, J. F. Quinn, E. Tjipto, F. Caruso and G. G. Qiao, *Macromolecules*, 2008, **41**, 2620–2626.
65 J. Ruths, F. Essler, G. Decher and H. Riegler, *Langmuir*, 2000, **16**, 8871–8878.
66 W.-M. Kulicke and C. Clasen, *Viscosimetry of Polymers and Polyelectrolytes*, Springer Verlag, Heidelberg, 2004.
67 H. P. Yap, X. Hao, E. Tjipto, C. Gudipati, J. F. Quinn, T. P. Davis, C. Barner-kowollik, M. H. Stenzel and F. Caruso, *Langmuir*, 2008, **24**, 8981–8990.
68 J. B. Gilbert, M. F. Rubner and R. E. Cohen, *Proc. Natl. Acad. Sci. U. S. A.*, 2013, **17**, 6651–6656.

69 E. Donath, D. Walther, V. N. Shilov, E. Knippel, A. Budde, K. Lowack, C. A. Helm and H. Möhwald, *Langmuir*, 1997, **13**, 5294–5305.
70 J. D. Mendelsohn, C. J. Barrett, V. V. Chan, A. J. Pal, A. M. Mayes and M. F. Rubner, *Langmuir*, 2000, **16**, 5017–5023.
71 Z. Sui and J. B. Schlenoff, *Langmuir*, 2003, **19**, 7829–7831.
72 S. A. Sukhishvili and S. Granick, *Macromolecules*, 2002, **35**, 301–310.
73 S. T. Dubas and J. B. Schlenoff, *Macromolecules*, 2001, **34**, 3736–3740.
74 E. J. Calvo and A. Wolosiuk, *J. Am. Chem. Soc.*, 2002, **124**, 8490–8497.
75 R. Waldmann, G. Champigny, E. Lingueglia, J. R. De Weille, C. Heurteux and M. Lazdunski, *Ann. N. Y. Acad. Sci.*, 1999, **868**, 67–76.
76 (*a*) K. Ariga, M. Li, G. J. Richards and J. P. Hill, *J. Nanosci. Nanotechnol.*, 2011, **11**, 1–13; (*b*) M. Ramanathan, L. K. Shrestha, T. Mori, Q. Ji, J. P. Hill and K. Ariga, *Phys. Chem. Chem. Phys.*, 2013, **15**, 10580–10611; (*c*) K. Ariga, M. V. Lee, T. Mori, X.-Y. Yu and J. P. Hill, *Adv. Colloid Interface Sci.*, 2010, **154**, 20–29; (*d*) K. Ariga, T. Mori and J. P. Hill, *Langmuir*, 2013, **29**, 8459–8471.
77 (*a*) J. Dai, A. M. Balachandra, J. Il Lee and M. L. Bruening, *Macromolecules*, 2002, **35**, 3164–3170; (*b*) S. Uk, R. Malaisamy and M. L. Bruening, *J. Membr. Sci.*, 2006, **283**, 366–372; (*c*) J. J. Harris, J. L. Stair and M. L. Bruening, *Chem. Mater.*, 2000, **12**, 1941–1946; (*d*) H. H. Rmaile, T. R. Farhat and J. B. Schlenoff, *J. Phys. Chem. B*, 2003, **107**, 14401–14406; (*e*) A. A. Antipov and G. B. Sukhorukov, *Adv. Colloid Interface Sci.*, 2004, **111**, 49–61; (*f*) A. A. Antipov, G. B. Sukhorukov, E. Donath and H. Möwald, *J. Phys. Chem. B*, 2001, **105**, 2281–2284; (*g*) G. B. Sukhorukov, A. L. Rogach, B. Zebli, T. Liedl, A. G. Skirtach, K. Köhler, A. A. Antipov, N. Gaponik, A. S. Susha and M. Winterhalter, *Small*, 2005, **1**, 194–200; (*h*) L. J. De Cock, S. De Koker, B. G. De Geest, J. Grooten, C. Vervaet, J. P. Remon, G. B. Sukhorukov and M. N. Antipina, *Angew. Chem., Int. Ed.*, 2010, **49**, 6954–6973.
78 J. A. De Feijter, J. Benjamins and F. A. Veer, *Biopolymers*, 1978, **17**, 1759–1772.
79 G. Z. Sauerbrey, *Z. Phys.*, 1959, **155**, 206–222.
80 W. Stober and A. Fink, *J. Colloid Interface Sci.*, 1968, **26**, 62–69.

 This journal is © the Owner Societies 2015